Talanta 84 (2011) 1005–1010

Contents lists available at ScienceDirect

Talanta

journal homepage: www.elsevier.com/locate/talanta

Special susceptive aqueous ammonia chemi-sensor: Extended applications of novel UV-curable polyurethane-clay nanohybrid

Sher Bahadar Khan[a,*], Mohammed M. Rahman[a], Eui Soung Jang[b], Kalsoom Akhtar[c], Haksoo Han[b,**]

[a] Centre for Advanced Materials and Nano-Engineering (CAMNE), Department of Chemistry and Faculty of Science and Arts, Najran University, P.O. Box 11001, Najran, Saudi Arabia
[b] Department of Chemical and Biomolecular Engineering, Yonsei University, 262 Seongsanno, Seodaemun-gu, Seoul 120-749, South Korea
[c] Division of Nano Sciences and Department of Chemistry, Ewha Womans University, Seoul 120-750, South Korea

ARTICLE INFO

Article history:
Received 12 January 2011
Received in revised form 21 February 2011
Accepted 23 February 2011
Available online 2 March 2011

Keywords:
Polyurethane acrylate (PU)
Cloisite 20B
Nanohybrid
Ammonia sensing

ABSTRACT

In this contribution, chemical sensor for the detection of aqueous ammonia has been fabricated using UV-curable polyurethane acrylate (PU) and nanohybrids (NH-1, NH-3 and NH-5). PU has been prepared by reacting polycaprolactone triol (PCLT) and isophorone diisocyanate (IPDI) while the nanohybrids, NH-1, NH-3, and NH-5 have been synthesized by solution blending method using PU with 1, 3, and 5 wt% loading levels of C-20B. PU and their nanohybrids showed higher sensitivity investigated by *I–V* technique using aqueous ammonia as a target chemical. All the nanohybrids showed higher sensitivity as compared to neat PU. The sensitivity increased with increase in clay content and the nanohybrid containing 5 wt% of clay showed the highest sensitivity (8.5254 μA cm^{-2} mM^{-1}) with the limit of detection (LOD) of 0.0175 ± 0.001 μM, being 7.8 times higher than pure PU. The calibration plot for all the sensors was linear over the large range of 0.05 μM to 0.05 M. The response time of the fabricated sensor was <10.0 s. Therefore, one can fabricate efficient aqueous ammonia sensor by utilization of nanohybrid as an efficient electron mediator.

1. Introduction

Environmental pollution is one of the serious problem introduced by thermal process, agricultural runoff and effluents discharged by industries. These environmental pollution attracted the attention of environmentalists, technologists, and others [1,2]. Ammonium hydroxide is the common pollutant which effects the environment due to their toxic, hazardous, corrosive and polluting nature. Ammonium hydroxide has toxic nature and cause lung disease, burning of skin and permanent blindness [3–5]. Hence for environmental safety, early detection of ammonium hydroxide is needed [5]. A lot of efforts have been devoted to the development of sensitive chemical sensor but most of the chemical sensors are only concerned about the detection of ammonia in gas phase. Detection of ammonia in solution phase is desirable for industrial and environmental applications and therefore, solution phase ammonia sensors have attracted significant attention to detect low level of ammonia solution in environment at room temperature [6–9].

Metal oxide nanostructures have widely been used as a chemical sensors for the detection of ammonia but all these materials are synthesized by hydrothermal methods at high temperature [10,11]. Here we are introducing PU synthesized by UV-curing technology which has gained increasing interest due to their environmental safety. UV-curing technology have advantage over thermal curing because of low energy consumption, high curing speed, cost efficient, low temperature and enhanced performance [12–15]. Due to environmental pollution, thermal curing technology losses their importance because of its high energy consumption, low curing speed and a lot of gasses and effluents discharge to the environment. As it has interesting physical and chemical properties, being an attractive material for many applications [12–19], it is needed to improve its sensing properties. We made an attempt to fabricate PU and PU/organoclay nanohybrids to improve their sensing properties and extend their usage as sensors.

Clay has wide range of applications in catalysis, sensing, drug delivery and polymer/clay nanocomposites. Polymer/clay nanocomposites present unusual properties especially enhanced anti-water sorption, thermal, mechanical and sensing properties [20]. Clay plays an important role in the environmental sciences as an electrode modifier because of their ion exchange property [21]. This application is particularly useful for the development of electrochemical sensors because they can accumulate electroactive ions within the clay layer. Delamination of clay plays an impor-

* Corresponding author. Tel.: +966 593541984.
** Co-corresponding author.Tel: +82-2 312 1417; Fax: +82 2 312 6401.
E-mail addresses: drkhanmarwat@gmail.com (S.B. Khan), hshan@yonsei.ac.kr (H. Han).

0039-9140/$ – see front matter © 2011 Elsevier B.V. All rights reserved.
doi:10.1016/j.talanta.2011.02.036

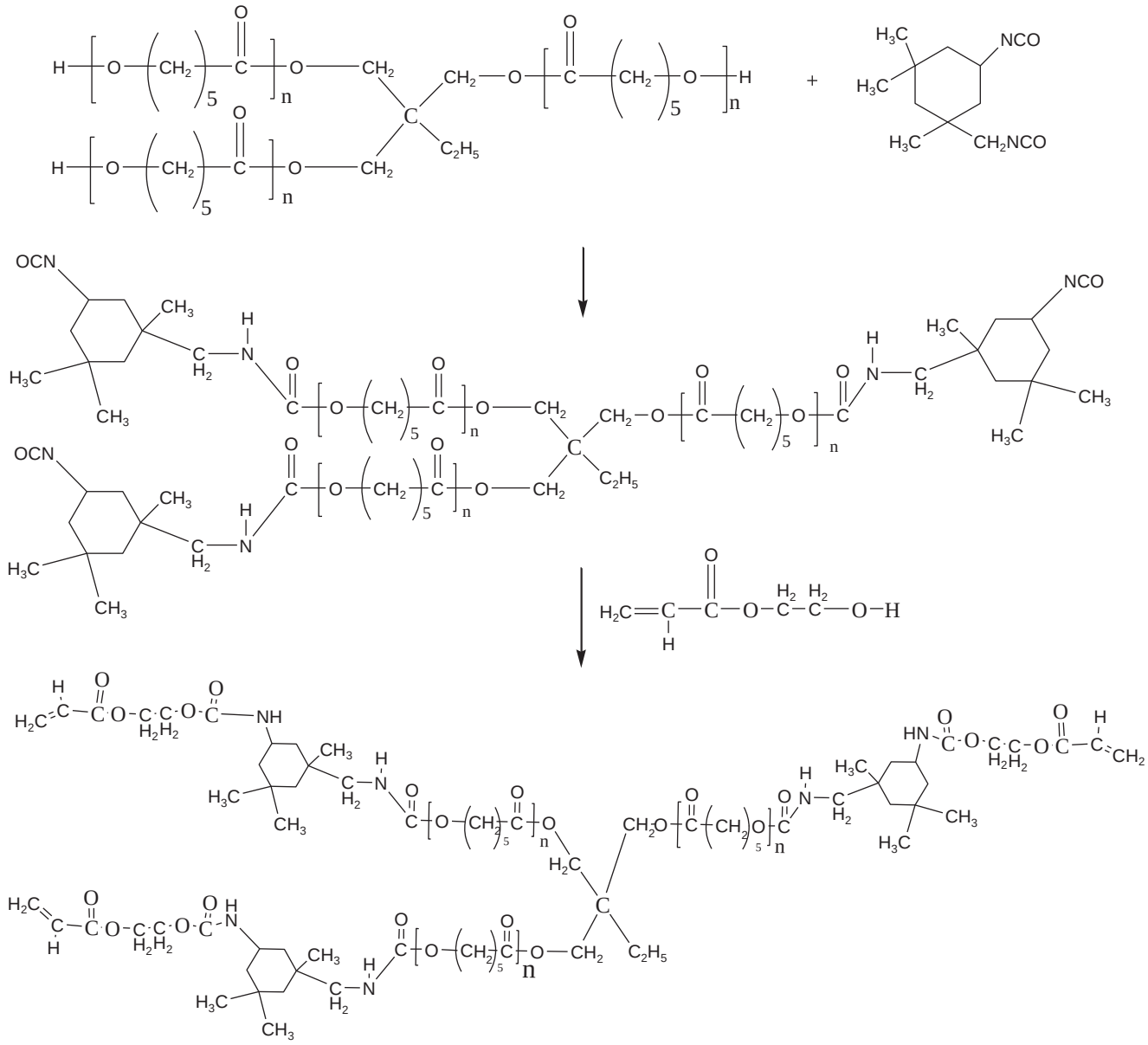

Scheme 1. Synthetic pathway of polyurethane acrylate.

tant role in charge transport. Various methods have been used for the achievement of delamination of clay, one of that is intercalation of molecules (surfactants or polymers). Nanocomposition of conductive polymer with clay also enhances charge transport [20].

In this contribution, PU and PU/C-20B nanohybrids with 1, 3, and 5 wt% clay loadings were synthesized and characterized by FT-IR spectroscopy, X-ray diffraction (XRD) and transmission electron microscopy (TEM). PU and PU/C-20B nanohybrids were then applied for ammonia sensing which is very important from application point of view in environmental science.

2. Experimental

The entire chemicals such as closite 20B, monosodium phosphate, disodium phosphate, ammonia solution (25%), dibutyltin dilaurate (DBT, Mw: 631.56 g/mol), polycaprolactone triol (PCLT, average Mn: 900 g/mol) and polyol, 2-hydroxyethyl acrylate (2-HEA, Mw: 116.12 g/mol) were purchased from Aldrich. TCI Korea provided isophorone diisocyanate (IPDI, Mw: 222.28 g/mol) while the trimethylolpropane triacrylate (TMPTA, Mw: 296.32 g/mol) was purchased from Miwon Commercial Co. Ltd. (Korea). The photoinitiator, 1-hydroxycyclohexyl phenyl ketone (Irgacure 184 D, Mw: 204.26 g/mol) was purchased from Ciba Specialty Chemicals. All the chemicals were of reagent grade and used without further purification. Double distilled water was used throughout the study. The chemical structure of trifunctional polyols used in this study is shown in Scheme 1.

In a typical PCLT-IPDI (hyperbranched urethane acrylate oligomer) synthesis process, 1.0 mol of PCLT was added to 2.5 mol of IPDI and mixed perfectly by mechanical stirring at 80 °C for 3 h. 2HEA was then added drop wise at same temperature and maintained the stirring for further 2 h. The resulting mixture was cooled down to 60 °C and approximately 200 ppm of DBT was added and continued the stirring for additional 2 h. At last, tipping of NCO-termination was carried out by 1 h stirring with HEA at below 60 °C (Scheme 1). The mixture of urethane acrylates, 5 wt% photoinitiator, TMPTA and MMA (methyl metacrylate) was heated slightly above an ambient temperature and mixed homogeneously, fol-

lowed by casting on a glass plate. UV-curing was carried out by exposing samples to metal halide UV lamp (1000 W/cm), high pressure mercury UV lamp (1000 W/cm), and finally metal halide UV lamp (1000 W/cm) for 30 s, respectively [14]. After peeling off from the glass plate, the cured films were stored in desiccators at room temperature for further studies.

Nanohybrids (PU/C-20B) with three different composition (99/1, 97/3 and 95/5) were synthesized by solution intercalation method. First, PU was dissolved in 30 ml of MMA followed by drop wise addition of dispersed solution of C-20B (C-20B in MMA). The resulting solution was stirred for 24 h at room temperature [14]. After terminating the reaction, the resulting precipitate was casted on a glass plate and cured by UV. Films of ~2 mm thickness were used to test the properties.

For the detection of ammonium hydroxide by *I–V* technique, a cell is constructed consisting film of PU and all nanohybrids as a working electrode (directly) and Pd wire is used a counter electrode. Ammonium hydroxide (25%) solution is diluted at different concentrations in DI water and used as a target chemical. Amount of 0.1 M phosphate buffer solution was kept constant as 20.0 ml throughout the investigation. Solution is prepared with various concentrations of ammonium hydroxide from 0.05 μM to 5.0 M. The sensitivity is calculated from the ratio of voltage and current of the calibration plot. 0.1 M phosphate buffer solution is used at pH 7.0 which has been prepared by mixing 0.2 M Na_2HPO_4 and 0.2 M NaH_2PO_4 solution in 100.0 ml de-ionized water.

The characterizations of all samples were carried out by using various techniques. The composition of the synthesized PU and nanohybrids were analyzed by Fourier transform infrared spectrometer (FT-IR) (Excalibur Series FT-IR). The structural characterizations were performed by X-ray diffraction (XRD) pattern by using Rigaku diffractometer using the Ni-filtered Cu-K_α1 radiation (λ = 1.5405 Å). The general morphologies of the synthesized nanohybrids were examined by transmission electron microscopy (TEM) by using LIBRA 120 energy-filtering transmission electron microscope (EF-TEM). The samples for TEM study were prepared by dissolving the sample in ethanol and a carbon–copper grid was dipped into the mixture. Then the sample adhering on the grid was cured by UV. Chemical sensing performance of PU and nanohybrids was analyzed by electrometer (Kethley, USA) using *I–V* technique in two electrode system.

3. Results and discussion

Spectral investigations of the synthesized PU are in accordance with the proposed structure. Polymerization of monomers was confirmed by the disappearance of the sharp NCO vibration at 2265 cm^{-1}. Fig. 1 (PU) shows the typical FTIR spectra of the UV-cured polyurethane acrylate. PU showed absorption band at 3390, 2900, 1720, 1530 and 1100 cm^{-1} [14]. These absorption bands for pure PU are due to stretching vibration of N–H, C=O, C–N, C–O and C–H.

In the spectrum of the C-20B (Fig. 1), the absorption bands at 1050 and 914 cm^{-1} results from stretching vibrations of Si–O and Al–Al–OH stretching mode in octahedral layer [14,20]. The peaks for silanol groups appeared in the region of 3400–3600 cm^{-1} [20] while the peaks appeared at 2926, 2852 and 1470 cm^{-1} are due to C–H stretching vibrations of CH_3, CH_2 and CH_2 bending, respectively which come from the alkylammonium present in the organophilic clay [14,20].

FT-IR spectra of NH-1, NH-3 and NH-5 are depicted in Fig. 1. All the characteristic peaks of clay and PU were detected in the spectrum of NH-1, NH-3 and NH-5, suggesting the formation of nanohybrids. The characteristic absorption bands appeared in the nanohybrids spectra are due to stretching vibration of N–H at 3400–3350 cm^{-1}, C=O at 1720 cm^{-1}, C–N at 1530 cm^{-1}, C–O at

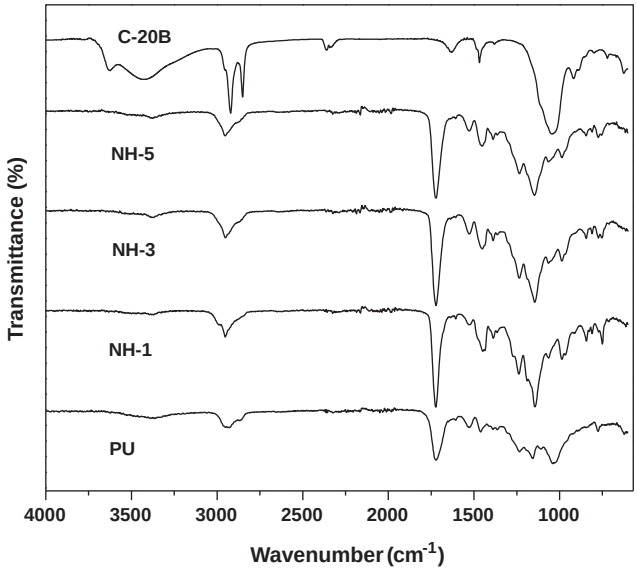

Fig. 1. Typical FT-IR spectra of (a) NH-5, (b) NH-3, (c) NH-1, (d) PU, and (e) C-20B.

1100 cm^{-1}, and C–H at 2800–2900 cm^{-1}. The data is in good agreement with the data reported by Bonilla et al. [14,20,22].

The quality, structural geometry and nanohybrid formations were investigated by X-ray diffraction (Fig. 2) which generally presents information about the increase in basal spacing of organoclays used. C-20B was used in order to get nanohybrids with improved ammonia sensing property. C-20B is an organoclay having increased basal spacing and organophilic character and thus PU can more easily enter into the sheet of the clay. The basal spacing of the clay and synthesized nanohybrids were calculated from the d_{001} peak using the Bragg's equation. XRD spectrum of C-20B shows an intense peak at 27.4 Å which shift to 40.1 Å after treatment with PU in acetone at room temperature. The XRD curves of NH-1, NH-3 and NH-5 shifted to lower 2θ values of 2.32, corresponding to a basal spacing of 38.05 Å. These significant increase in the basal space confirm that PU chains have been intercalated into the sheets of the clay and increased the basal spacing of the sheets. When clay loading level is high, a more obvious peak appears in the XRD patterns which may be due to the higher amount of clay [14,20].

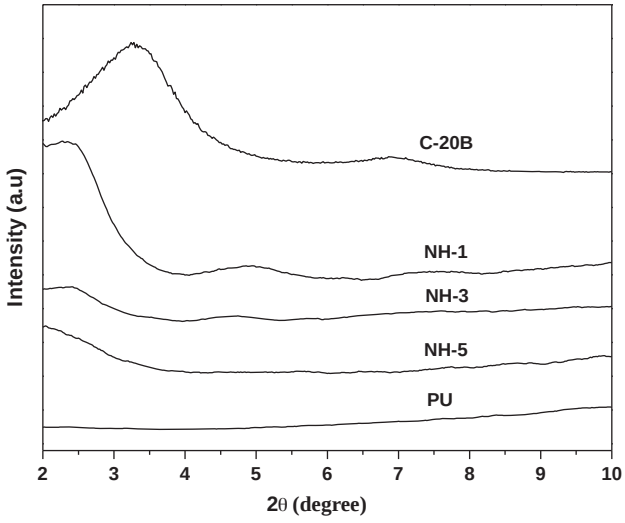

Fig. 2. Typical powder XRD patterns of (a) NH-5, (b) NH-3, (c) NH-1, (d) PU, and (e) C-20B.

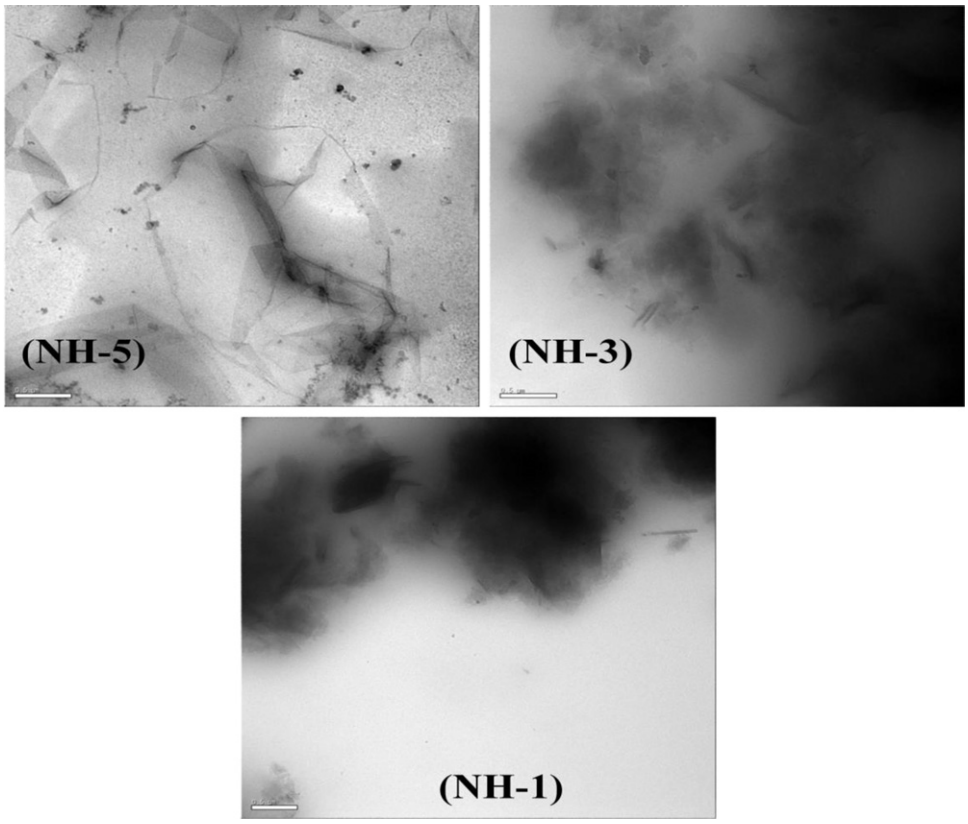

Fig. 3. TEM images of (a) NH-5, (b) NH-3 and (c) NH-1.

Fig. 3 shows the typical TEM micrograph of NH-1, NH-3 and NH-5. TEM images shows that PU chains are successfully intercalated into the layer of C-20B. TEM images confirm that NH-1 and NH-3 exhibit intercalated morphology whereas NH-5 shows partially delaminated structure. NH-1 and NH-3 images show that C-20B exist in stacked and flocculated form in PU matrix (Fig. 3), whereas NH-5 image shows 5–10 multilayer aggregates of C-20B in polymer matrix. NH-5 shows the highest degrees of nano-dispersion in PU and thus has a higher level of delamination and a better degree of dispersion in PU nanohybrid than NH-1 and NH-3. Examinations of many TEM images confirm that the degree of clay dispersion in the PU nanohybrids follow the order: 5 wt% > 3 wt% > 1 wt%. Thus it is found that with increasing C-20B content, the dispersibility of clay increases and aggregation decrease. The data is in good agreement with the data reported by Zhang et al. [14,23].

The PU, NH-1, NH-3 and NH-5 were employed for the detection of ammonia in liquid phase. The thin film of PU, NH-1, NH-3 and NH-5 was used as working electrode where ammonium hydroxide was selected as a target chemical. The electrical response of ammonia has been measured using *I–V* technique [11,24–26]. Fig. 4(a) shows electrical response of the NH-5 thin film without ammonium hydroxide (gray-dotted line) and with 100.0 μl ammonium hydroxide (dark-dotted line) in 0.1 M phosphate buffer solution (pH 7.0). The pH of the solution is kept constant because increase in pH affects the efficiency of the electrochemical experiment which may be due to the increase in ion carriers [27].

It is observed from Fig. 4(a) that by injecting the target chemical, PU shows a significant increase in the electrical current which reflects the sensitivity of PU to ammonium hydroxide [11,24]. Thus by injection of ammonium hydroxide, increase in electrical response suggests that PU has rapid and sensitive response to the target chemical. The fast electron exchange and good electro-catalytic oxidation properties are responsible for the high electrical response of PU sensor to ammonium hydroxide [11,24].

The standard electrode potential (E^0) of NH_4OH is equal to zero and thus easily undergoes catalytic dissociation reaction by applying to *I–V* technique as shown in Eq. (1). The catalytic reaction of NH_4OH produces NH_4^+ and OH^- (increase the carrier ions) which increases the conductivity of the host material by providing excess electron to the conduction band of the material [24].

$$NH_4OH \rightarrow NH_4^+ + OH^- \quad (1)$$

According to the microscopic model reported earlier [28–30], the subsequent emission of an electron takes place from the chemisorbed oxygen species into the conduction band of the sensor and cause change in the electrical conductance of sensor. Mechanistically, atmospheric oxygen molecules physically adsorb on the surface and produces anion O_{ads}^- (O^- or O_2^-) (Eq. (2)) by extracting an electron from the conduction band of the sensor. This O_{ads}^- react with ammonium ion produced by the catalytic reaction of ammonium hydroxide and discharge the trapped electron to the conduction band of PU and enhances the conductivity of PU.

$$O_2 + 2e^- \rightarrow 2O_{ads}^- \quad (2)$$

The concentration of ammonia was varied from 0.05 μM to 5.0 M by adding de-ionized water to liquor ammonia in different proportions and investigated the effect of ammonium hydroxide concentration on the electrical response of PU thin film. Ammonium hydroxide was successively added in the range of 0.05 μM to 5.0 M into continuously stirred 0.1 M PBS solution (pH 7.0) and the graph is depicted in Fig. 3(b). Each *I–V* response of PU to varying concentration of liquor ammonia shows current of PU as a function of ammonium hydroxide concentration at room temperature. It is observed that at lower to higher concentration of target compound, the current increases gradually. Increasing electrical current

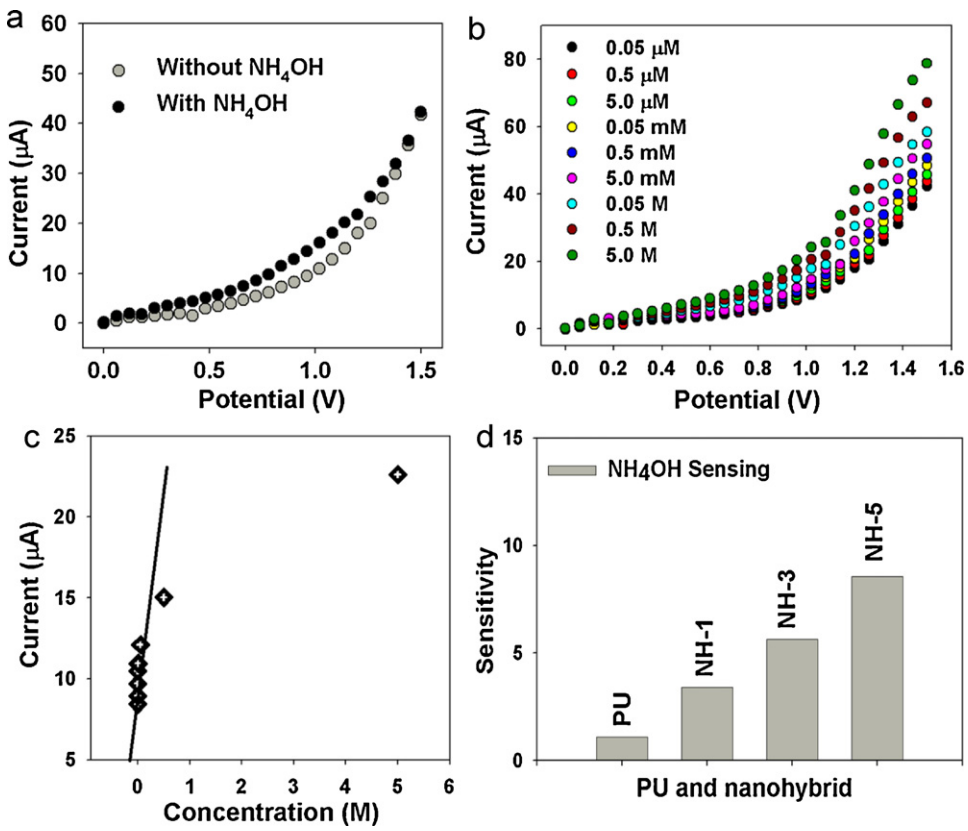

Fig. 4. *I–V* curves of (a) with and without ammonium hydroxide, (b) concentration variation of ammonium hydroxide, (c) calibration curve of ammonium hydroxide using NH-5, and (d) comparison of sensitivity.

with increasing ammonium hydroxide concentration indicates that with increase in the concentration of ammonium hydroxide, the PU film conductivity increased which is ascribed to the increase in ions providing excess electron to the conduction band of the material [11,24–27].

Fig. 4(c) shows the corresponding calibration curve of the PU sensor which is plotted from the variation of target concentration. Initially current response increases as the concentration of ammonium hydroxide increases and after certain concentration electrical response become constant and thus saturation takes place at high concentration above 0.05 M. Calibration curve depicts two sensitivity regions; region at lower concentrations is linear up to 0.05 M with correlation coefficient (R) of 0.6223. The sensitivity is calculated from the slope of the lower concentration region of calibration curve, which is 1.0901 $\mu A\,cm^{-2}\,mM^{-1}$. The linear dynamic range of this sensor exhibits from 0.05 μM to 0.05 M and the detection limit was estimated, based on signal to noise ratio (S/N), to be 0.031 ± 0.001 μM. Above 0.05 M concentration the sensor become saturated. This sensor shows higher sensitivity at low concentration region and would be useful at lower ammonium hydroxide concentration at room temperature. The saturation region at higher concentration might be due to the unavailability of free PU sites for ammonium hydroxide adsorption. The higher sensitivity of PU at lower concentration is due to availability of the free surface for physisorption process which plays a major role in sensitivity of the sensor. The saturation of the sensor takes place due to chemisorption process which remains dominant at higher concentration and effects the sensor performance [11,24].

To check the effect of clay on the performance of PU for the detection of ammonia, NH-1, NH-3 and NH-5 were studied as a chemical sensor for ammonium hydroxide detection. NH-1, NH-3 and NH-5 based ammonia sensor showed sensitivity of 3.4103, 5.6485 and 8.5254 $\mu A\,cm^{-2}\,mM^{-1}$ with a response time <10 s. The sensing results demonstrate that NH-5 shows the highest sensitivity with low detection limit (0.0175 ± 0.001 μM) which was

Table 1
Sensing performance of PU and PU/C-20B nanohybrids and their comparison with other nanocomposites in literature.

Analyte	Clay	LoD (μM)	Sensitivity ($\mu A\,cm^{-2}\,\mu M^{-1}$)	Reference
PU	Cloisite 20 B (5 wt%)	0.0175	8.5254	Present work
PU	Cloisite 20 B (3 wt%)	–	5.6485	Present work
PU	Cloisite 20 B (1 wt%)	–	3.4103	Present work
PU	–	0.031	1.0901	Present work
Fe^{3+}	Montmorillonite	4.0	–	32
Cu^{2+}	Laponite	80.0	–	33
Ca^{2+}	Montmorillonite	4.0	–	34
Methyl viologen	Laponite	5.0	–	35
Nitrobenzene	Sepiolite	1.6	–	36
Amitrole	Nontronite	3.0	–	37
Lactate	Laponite	1.0	–	38

estimated based on signal to noise ratio (S/N) (Fig. 4(d)). Thus the nanohybrid containing 5 wt% of clay significantly increased the sensitivity (8.5254 $\mu A\,cm^{-2}\,mM^{-1}$) which is 7.8 times higher than that of pure PU (1.0901 $\mu A\,cm^{-2}\,mM^{-1}$). Similarly the introduction of 1 and 3 wt% of clay into PU increased the sensitivity of PU from 1.0901 $\mu A\,cm^{-2}\,mM^{-1}$ to 3.4103 and 5.6485 $\mu A\,cm^{-2}\,mM^{-1}$, respectively. The increase in sensitivity of PU by addition of clay may be due to the accretion of electroactive ions within the clay layer which can act as matrices for electroactive ions because they are usually able to incorporate ions by an ion-exchange process. Further the highest sensitivity of NH-5 may be due to high concentration and delamination of clay within the polymer matrix which enhance charge transport and increase the electrical response [21].

In addition to this, performances of NH-5 based aqueous ammonia sensors was compared with the previously reported nanocomposites and summarized in Table 1. NH-5 showed much higher sensitivity and lower detection of limit than those of previously reported ammonia sensors [31–37]. Moreover, it can be considered that the clay delamination plays an important role in the performance of the sensors. Therefore, one can conclude that the PU nanohybrid with 5 wt% of C-20B is a good candidate, compared to other polymers and nanomaterials for the fabrication of efficient and highly sensitive aqueous ammonia sensors.

4. Conclusion

PU and PU/C-20B nanohybrids with various clay contents were prepared and characterized by FTIR, XRD and TEM. Both PU and nanohybrids were applied for aqueous ammonia sensing using *I–V* technique and studied the electrical behavior at different NH_4OH concentrations. Nanohybrids showed higher sensitivity and lower LOD value as compared to PU which indicates that the sensing property of PU was improved by adding C-20B into PU matrix. Thus nanohybrid provides an efficient way to improve the sensing property of PU to widely expand its application and consequently can make suitable sensor for use in chemical industries.

Acknowledgments

This work was supported by the National Research Foundation of Korea Grant Funded by the Korean Government (MEST) (NRF-2009-C1AAA001-0092926) and New & Renewable Energy R&D Program (2009100100606) under the Ministry of Knowledge Economy, Republic of Korea. Centre for Advanced Materials and Nano-Engineering (CAMNE) and Deanship of Scientific Research, Najran University, Najran is highly acknowledged.

References

[1] E.J. Wolfrum, R.M. Meglen, D. Petersona, J. Sluiter, Sens. Actuators B 115 (2006) 322–329.
[2] A.O. Dikovska, G.B. Atanasova, N.N. Nedyalkov, P.K. Stefanov, P.A. Atanasov, E.I. Karakolev, A.T. Andreev, Sens. Actuators B 146 (2010) 331–336.
[3] D. Leduc, P. Gris, P. Lheureux, P.A. Gevenois, P.D. Vuyst, J.C. Yernault, Thorax 47 (1992) 755–757.
[4] S. Banerji, W. Peng, Y.C. Kim, N. Menegazzo, K.S. Booksh, Sens. Actuators B 147 (2010) 255–262.
[5] M.M. Rahman, A. Jamal, S.B. Khan, M. Faisal, J. Nanopart. Res. (2011), doi:10.1007/s11051-011-0301-7.
[6] G. Ballun, F. Hajdu, G. Harsanyi, Elect. Tech. (2003) 471–475.
[7] C.Y. Shen, S.Y. Liou, Sens. Actuators B 131 (2008) 637–679.
[8] S. Christie, E. Scorsone, K. Persaud, F. Kvasnik, Sens. Actuators B 90 (2003) 163–169.
[9] V.B. Raj, A.T. Nimal, Y. Parmar, M.U. Sharma, K. Sreenivas, V. Gupta, Sens. Actuators B 147 (2010) 517–524.
[10] P. Guo, H. Pan, Sens. Actuators B 114 (2006) 762–767.
[11] M. Faisal, S.B. Khan, M.M. Rahman, A. Jamal, Mater. Lett. (2011), doi:10.1016/j.matlet.2011.02.013.
[12] S. Simic, B. Dunjic, S. Tasic, B. Bozic, D. Jovanovic, I. Popovic, Prog. Org. Coat. 63 (2008) 43–48.
[13] E. Dzunuzovic, S. Tasic, B. Bozic, D. Babic, B. Dunjic, Prog. Org. Coat. 52 (2005) 136–143.
[14] E.S. Jang, S.B. Khan, H. Han, Prog. Org. Coat. (2011), doi:10.1016/j.porgcoat.2010.12.007.
[15] J. Zhu, F.M. Uhl, A.B. Morgan, C.A. Wilkie, Chem. Mater. 13 (2001) 4649–4654.
[16] J. Lange, E. Stenroos, M. Johansson, E. Malmstrom, Polymer 42 (2001) 7403–7410.
[17] C. Ha, S. Jung, E. Kim, W. Kim, S. Lee, J. Cho, J. Appl. Polym. Sci. 62 (1996) 1011–1021.
[18] V.D. Athawale, M.A. Kulkarni, Prog. Org. Coat. 65 (2009) 392–400.
[19] X. Chen, Y. Hu, L. Song, C. Jiao, Polym. Adv. Technol. 19 (2009) 322–327.
[20] S.B. Khan, J. Seo, E.S. Jang, J.S. Choi, S. Choi, H. Han, Membr. J. 19 (2009) 341–347.
[21] C. Mousty, Appl. Clay Sci. 27 (2004) 159–177.
[22] G. Bonilla, M. Martinez, A.M. Mendoza, J.M. Widmaier, Eur. Polym. J. 42 (2006) 2977–2986.
[23] Z. Zhang, Q. Shi, J. Peng, J. Song, Q. Chen, J. Yang, Y. Gong, R. Ji, X. He, J.H. Lee, Polymer 47 (2006) 8548–8555.
[24] S.G. Ansari, Z.A. Ansari, H.K. Seo, G.S. Kim, Y.S. Kim, G. Khang, H.S. Shin, Sens. Actuators B 132 (2008) 265–272.
[25] S.G. Ansari, R. Wahab, Z.A. Ansari, Y.S. Kim, G. Khang, A. Al-Hajry, H.S. Shin, Sens. Actuators B 137 (2009) 566–573.
[26] S.G. Ansari, Z.A. Ansari, R. Wahab, Y.S. Kim, G. Khang, H.S. Shin, Biosens. Bioelectron. 23 (2008) 1838–1842.
[27] A. Umar, M.M. Rahman, S.H. Kim, Y.B. Hahn, Chem. Commun. (2008) 166–168.
[28] W. Henry, M. Peter, J. Electrochem. Soc. 126 (1979) 627–633.
[29] N.J. Dayan, S.R. Sainkar, R.N. Karekar, R.C. Aiyer, Thin Solid Films 325 (1998) 254–258.
[30] S.G. Ansari, P. Boroojerdian, S.R. Sainkar, R.N. Karekar, R.C. Aiyer, S.K. Kulkarni, Thin Solid Films 295 (1997) 271–276.
[31] J. Wang, T. Martinez, Electroanalysis 1 (1989) 167–170.
[32] D. Barancok, J. Cirak, P. Tomcık, K. Gmucova, Bioelectrochemistry 55 (2002) 153–155.
[33] S.H. Wang, T.C. Chou, Electroanalysis 12 (2000) 468–470.
[34] M. Pecorari, P. Bianco, Electroanalysis 10 (1998) 181–186.
[35] E. Lorenzo, E. Alda, P. Hernandez, M.H. Blanco, L. Hernandez, J. Anal. Chem. 330 (1988) 139–142.
[36] J.M. Zen, H.P. Chen, A.S. Kumar, Anal. Chim. Acta 449 (2001) 95–102.
[37] S. Cosnier, K.L. Lous, J. Electroanal. Chem. 406 (1996) 243–246.